Decentralized Opinion Integrated Decision making at Unsignalized Intersections via Signed Networks

Decentralized Opinion Integrated Decision Making at Unsignalized Intersections via Signed Networks

Bhaskar Varma, *Graduate Student Member, IEEE*, Ying Shuai Quan, Karl D. von Ellenrieder, *Senior Member, IEEE*, and Paolo Falcone

***Abstract*—In this letter, we consider the problem of decentralized decision making among connected autonomous vehicles (CAVs) at unsignalized intersections. We propose a safe closed-loop opinion-driven decision making model for intersection coordination, where vehicles exchange intent through dual signed networks: a conflict topology based communication network and a commitment-driven belief network, enable cooperation without a centralized coordinator. Continuous opinion states modulate velocity optimizer weights prior to commitment; a closed-form predictive feasibility gate then freezes each vehicle's decision into a GO or YIELD commitment, which propagates back through the belief network to precondition neighbor behavior ahead of physical conflicts. On average, our policy outperforms both the First-Come-First-Served Policy and a conflict-aware predictive safety gate, with the largest gains observed when feasible gaps arise from heterogeneous conflict sets.**

***Index Terms*—Autonomous vehicles, decentralized control, cooperative control, transportation networks.**

I. Introduction and Related Work

UNSIGNALIZED urban intersections represent one of the most demanding coordination environments for connected autonomous vehicles (CAVs). While the problem is not new and may appear to be solved using centralized model predictive control (MPC) [1], the main issue is that it relies on a centralized coordinator and considers only longitudinal control along straight paths, a limitation that persists even in decentralized MPC (DMPC) extensions [2]. Reservation-based methods [3] treat the intersection as a shared resource and assign time slots through a centralized intersection manager. Some intersection managers propose a First Come First Served (FCFS) policy [4], instead of an optimal passing order. This works adequately if one only considers straight-path maneuvers, but with turn maneuvers the overall throughput will be compromised. Recent approaches take the lane geometry and turns into consideration [5], but again reintroduce a centralized controller, which increases the computational complexity and dependence when upscaled. Also, learning-based optimization algorithms have been proposed [6], yet remain dependent on offline training and generalize poorly across unseen configurations. These approaches either require a persistent central authority that fails to scale gracefully under coordinator failure or intermittent communication, or rely on optimization-based joint and distributed MPC formulations that achieve strong performance at the cost of computational complexity.

On the other hand, opinion dynamics [7] have recently attracted attention, especially for decentralized, interactive decision making, including robots interacting with human movers in [8], task allocation in uncrewed surface vessels [9], and unsignalized roundabouts [10]. Opinion dynamics on signed social networks [11] offer a different paradigm: distributed agents form opinions through local interactions, and bifurcation phenomena naturally produce differentiated equilibria without explicit negotiation. The natural bifurcation of signed-network equilibria into two opposing committed states maps directly onto the binary GO/YIELD decision required at intersections. The multi-topic extension in [12] establishes conditions under which structurally balanced signed networks produce stable committed equilibria.

The primary focus of this work is to study interactive decision making at intersections, not throughput maximization as in high-density traffic management. While extensive literature addresses the latter, the core problem of individual vehicle decision-making is often bypassed through centralized sequencing, rather than by vehicles resolving it distributively. In general, opinion dynamics are used for group decision making, where agents collectively converge to a shared opinion. However, with no mechanism to prevent two conflicting vehicles from simultaneously deciding to cross, they cannot guarantee safety at an intersection. We address this gap by

Received 17 March 2026; revised 18 May 2026; accepted 4 June 2026. Date of publication 17 June 2026; date of current version 30 June 2026. This article has not been presented at a conference. Recommended by Senior Editor I.-C. Morarescu. *(Corresponding author: Bhaskar Varma.)*

Bhaskar Varma and Karl D. von Ellenrieder are with the Faculty of Engineering, Free University of Bozen-Bolzano, 39100 Bolzano, Italy (e-mail: sbalagopala@unibz.it; karl.vonellenrieder@unibz.it).

Ying Shuai Quan and Paolo Falcone are with the Mechatronics Group, Department of Electrical Engineering, Chalmers University of Technology, 412 96 Gothenburg, Sweden (e-mail: quany@chalmers.se; paolo.falcone@chalmers.se).

Digital Object Identifier 10.1109/LCSYS.2026.3704463

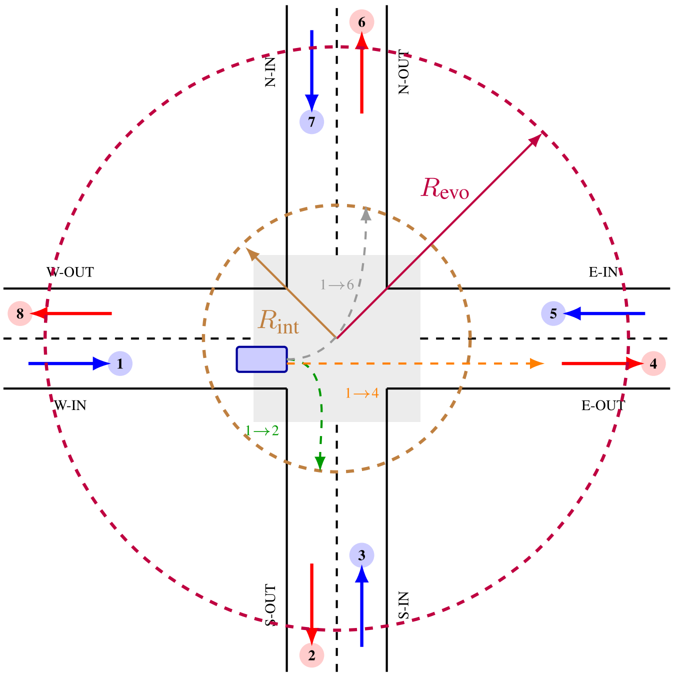

Fig. 1. Four-way unsignalized intersection. In-lanes (blue, labeled 1,3,5,7) and out-lanes (red, labeled 2,4,6,8). Maneuvers from lane 1: right turn 1 → 2 (green), straight 1 → 4 (orange), left turn 1 → 6 (gray). Red circle: evolution zone $R_{\text{evo}} = 15$ m.

proposing a closed loop decision making model, which treats each vehicle as an individual decision maker receiving group feedback used to make safe decisions. This letter makes the following contributions:

1) **Dual signed graph architecture.** A conflict based communication graph and commitment driven belief network together define structured Suppression, Permission, and Coordination channels, routing committed states through opinion dynamics without a weighted coupling matrix.
2) **Decomposed predictive coordination.** MPC is decomposed into a closed-form predictive feasibility check, which drives a commitment gate providing feedback to the opinion dynamics and a single-step multi-objective velocity optimizer, while preserving predictive safety.
3) **Opinion-integrated control.** The continuous opinion modulates optimizer weights, each commitment event updates the belief network, triggering opinion spikes that propagate intent back through the network.

II. Problem Statement

A. Intersection Geometry

We consider a four-way unsignalized intersection with right-hand traffic rules, as shown in Fig. 1. Each approach (West, South, East, North) has two lanes: an in-lane for approaching vehicles and an out-lane for departing vehicles. In-lanes are labeled $1, 3, 5, 7$ (West, South, East, North) and out-lanes $2, 4, 6, 8$ respectively.

B. Problem Statement

Given a set of CAVs approaching a four-way unsignalized intersection with mixed maneuver intentions, design a distributed coordination system such that:

(1) **Safety:** all vehicles complete their intended maneuvers without collision;
(2) **Decentralization:** without a central coordinator or pre-assigned crossing order.

C. Vehicle Model and Path Execution

Consider N_a CAVs with state $\mathbf{x}_i = [x_i, y_i, \theta_i, v_i]^\top$. Each vehicle follows a pre-computed arc-length parameterized path determined by its declared (in-lane, out-lane) intention. Path tracking is assumed ideal, The coordination layer determines $\dot{v}_i = a_i(t)$; path geometry serves as a fixed spatial reference along which each vehicle progresses. The length of each vehicle L_v is 4.5m and the width is 1.8m for the simulations.

III. Method

A. Signed Opinion Dynamics Model

We build on the nonlinear opinion dynamics framework of [12], summarized here and adapted in Section III-E. Let $i, k \in \{1, \ldots, N_a\}$ be agents and $j, l \in \{1, \ldots, N_o\}$ be options. The N_a agents are on a signed network with adjacency matrix $A \in \mathbb{R}^{N_a \times N_a}$, with entries $a_{ik}{>}0$ denoting cooperative and $a_{ik}{<}0$ antagonistic interactions. The belief-system matrix $B \in \mathbb{R}^{N_a \times N_o}$ has entries g_{jl}, with $g_{jl}{>}0$ reinforcing and $g_{jl}{<}0$ opposing cross-option coupling. Let $z_{ij} \in \mathbb{R}$ be the opinion of agent i about option j, using $\tanh(\cdot)$ as the saturation function transforms the continuous-time dynamics

$$\tau \dot{z}_{ij} = -d\, z_{ij} + \tanh\big(\bar{u}\, I_{ij}\big) + b_{ij}, \tag{1}$$

where $z_{ij} \in [-1, 1]$ and the internal state I_i is

$$\begin{aligned} I_{ij} = {} & \alpha\, z_{ij} + \gamma \sum_{k \neq i} a_{ik}\, z_{kj} \\ & + \beta \sum_{l \neq j} g_{jl}\, z_{il} + \delta \sum_{k \neq i} \sum_{l \neq j} a_{ik}\, g_{jl}\, z_{kl}. \end{aligned} \tag{2}$$

Here $\tau{>}0$ is the opinion time constant, $d{>}0$ is resistance, $\bar{u}{\geq}0$ is scalar attention, and b_{ij} is external bias. The four governing parameters are: α (self-reinforcement), γ (inter-agent coupling via signed A), β (cross-option coupling via B), and δ (combined inter-agent and cross-option). The neutral state $z = 0$ undergoes a pitchfork bifurcation at a critical attention $\bar{u}^*$. Above $\bar{u}^*$ agents rapidly commit to non-neutral opinions as proven by [12], a property we exploit for vehicle coordination via zone-based attention.

B. Zone-Based Attention and Commitment Mechanism

The intersection region is partitioned into three zones according to each vehicle's distance from the intersection center (which is the origin), as shown in Fig. 1, where $r_i(t) = \|\mathbf{p}_i(t)\|$; $\mathbf{p}_i = [x_i, y_i]^\top$ is position of vehicle i

$$\text{zone}_i(t) = \begin{cases} \text{EVOLUTION} & r_i < R_{\text{evo}},\ R_{\text{evo}} = 15\,\text{m}, \\ \text{DECISION} & r_i \leq R_{\text{int}},\ R_{\text{int}} = 5\,\text{m}, \\ \text{EXITED} & r_i > R_{\text{int}}. \end{cases}$$

To apply the opinion dynamics of (1) to intersection coordination, we replace the scalar attention $\bar{u}$ with a zone-dependent gain that increases as each vehicle approaches the intersection. Since decision is individual, j is now binary and unique per agent giving $z_{ij} \to z_i$; the proposed attention $u_i(t)$ for vehicle i at time t is

$$u_i(t) = u_0(\text{zone}_i) + K_u\big(z_i - \tfrac{1}{2}\big)^2, \tag{3}$$

with $u_0 = 0.5$ (EVOLUTION), $u_0 = 1.5$ (DECISION), and $K_u = 2.0$, driving opinion formation analogous to the pitchfork bifurcation in (1). Each vehicle maintains a discrete commitment state

$$\sigma_i \in \{N,\ G,\ Y,\ E\}, \tag{4}$$

where the letters denote NEGOTIATE, GO, YIELD, and EXIT. Initially $\sigma_i = N$. Opinion evolves continuously while $\sigma_i = N$ in the evolution zone, with attention gain u_i increasing as the vehicle approaches the intersection. Upon entering the decision zone, the predictive gate evaluates FCFS priority and safety, thresholding the opinion discretely at decision zone. This commitment mechanism facilitates cooperative collision free passing, which is discussed in detail at Section III-F.

C. Conflict Topology Based Communication Network

We design A directly from vehicle maneuver intent to encode conflict structure into the signed network. For each vehicle pair (i, k) we compute a crossing conflict indicator

$$K(i,k) = \begin{cases} 1 & \text{paths geometrically cross,} \\ 0 & \text{otherwise,} \end{cases}$$

and a merge indicator

$$M(i,k) = \begin{cases} 1 & \text{out-lane}_i = \text{out-lane}_j, \\ 0 & \text{otherwise.} \end{cases}$$

Both crossing and merge conflicts require sequencing; M is maintained separately to distinguish the type of deferral in the velocity optimization layer. Hence we design the static signed adjacency matrix $A \in \{-1, 0, +1\}^{N_a \times N_a}$, such that

$$A(i,k) = \begin{cases} -1, & K(i,k) = 1 \text{ or } M(i,k) = 1, \\ +1, & K(i,k) = 0 \text{ and } M(i,k) = 0, \\ \ \ 0, & i = k. \end{cases} \tag{5}$$

When $A(i,k) = -1$ we have an antagonistic edge (conflict requires sequencing) and when $A(i,k) = +1$ we have a cooperative edge (no conflict). Since geometric conflict is symmetric, $A(i,k) = A(k,i)$ giving an undirected graph.

D. Commitment State Aware Belief System Network

To propagate commitment decisions as feedback into the opinion dynamics, we design a dynamic belief matrix $B(t) \in \{-1, 0, +1\}^{N_a \times N_a}$ between vehicles (replacing the option-space graph B of (1)) that encodes the current commitment state of each vehicle shared via V2V as seen in Fig. 2.

$$B(i,k) = \begin{cases} +1, & \sigma_i = \text{GO}, \\ -1, & \sigma_k = \text{YIELD}, \\ \ \ 0, & \text{otherwise.} \end{cases} \tag{6}$$

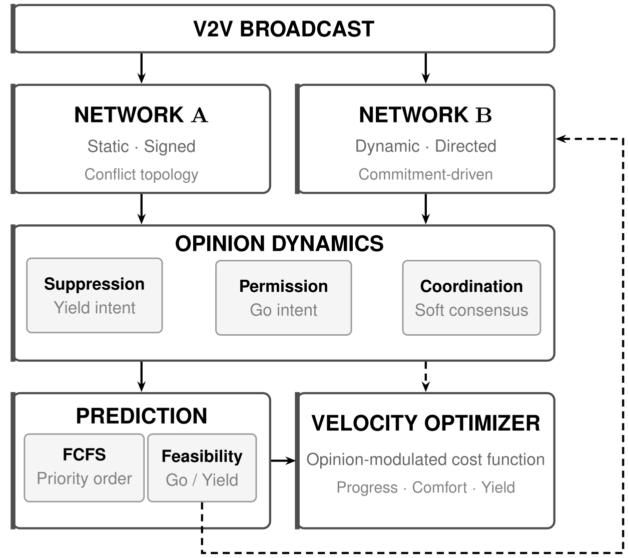

Fig. 2. Architecture of the proposed framework.

Unlike A, B is directed: $B(i,k) \neq B(k,i)$, since σ_i and σ_k evolve independently. And $B(i,k)$ is nonzero only when neighbor k has committed and is actively in the decision or intersection zone. An uncommitted neighbor ($B(i,k) = 0$) exerts no influence on i's opinion, preventing undecided vehicles from disrupting each other's opinion trajectories.

E. Safe Decision Making Model for Intersection

The opinion-dynamics in (1) are shifted from the range $[-1, 1]$ to $[0, 1]$ so $z_i = 0.5$ represents neutral, $z_i \to 1$ GO, $z_i \to 0$ YIELD, the reason for this is to nullify the yielded vehicle influence in the opinion evolution. The proposed individual decision dynamics model with group feedback is

$$\tau\, \dot{z}_i = -d\, z_i + \tfrac{1}{2}\big(1 + \tanh(u_i\, I_i)\big), \tag{7}$$

where $d = 1$, $\tau = 0.1$ s, here state $I_{ij} \to I_i$ as z_i is individual.

Instead of the internal state as in (2), Each neighbor k (i.e. $B(i,k) \neq 0$) is assigned to one of the three neighboring sets based on the joint state of $A(i,k)$ and $B(i,k)$ shown below:

$$\mathcal{N}_+^-(i) = \{j : A(i,k) = -1,\ B(i,k) = +1\},$$
$$\mathcal{N}_-^-(i) = \{j : A(i,k) = -1,\ B(i,k) = -1\},$$
$$\mathcal{N}^+(i) = \{j : A(i,k) = +1,\ B(i,k) \neq 0\}.$$

Then, depending upon which neighbor set vehicle k belongs to, we propose a three channeled signals influencing z_i as:

$$\textbf{Suppression:} \quad \mathcal{S}_i = \max_{j \in \mathcal{N}_+^-(i)} z_k,$$

where conflicting neighbor-committed GO drives $z_i \to 0$.

$$\textbf{Permission:} \quad \mathcal{P}_i = \text{mean}_{j \in \mathcal{N}_-^-(i)} (1 - z_k),$$

where conflicting neighbor-committed YIELD drives $z_i \to 1$.

$$\textbf{Coordination:} \quad \mathcal{C}_i = \text{mean}_{j \in \mathcal{N}^+(i)} z_k,$$

where cooperative neighbor committed GO/YIELD drives alignment. The internal state aggregating all 3 channels is

$$I_i = \alpha\big(z_i - \tfrac{1}{2}\big) - \alpha_S\, \mathcal{S}_i + \alpha_P\, \mathcal{P}_i + \alpha_C\, \mathcal{C}_i, \tag{8}$$

This is a key departure from (2), eliminating cross-option terms, β, δ, γ. Here, α is self gain and $\alpha_S > \alpha_P > \alpha_C$ are dedicated independent channel gains, introduced to govern channel influences. The gains satisfy $\alpha_S > \alpha_P + \alpha_C$, prioritizing conflict avoidance over cooperative alignment for safety. The proposed Internal state (8) makes the opinion dynamic model (7) closed loop: the belief matrix B, updated by the predictive gate, enters I_i through the channels, providing a continuous feedback from the intersection environment.

Proposition 1: (Properties of (7)): For any $z_i(0) \in (0, 1)$:

(i) $z_i(t) \in (0, 1)$ for all $t \geq 0$.

(ii) In the evolution zone ($u_i < u^*$), a unique globally asymptotically stable equilibrium $z_i^* \in (0, 1)$ exists $\forall\, B$

(iii) In the decision zone ($u_i > u^*$) with $B = \mathbf{0}$, $z_i = 0.5$ is unstable; for $B \neq \mathbf{0}$, $z_i = 0.5$ is not an equilibrium.

Proof: (i) Since $z_k \in (0, 1)$ by induction, the channel signals $\mathcal{S}_i, \mathcal{P}_i, \mathcal{C}_i \in [0, 1]$ are bounded, such that I_i is finite for all $z_i \in [0, 1]$. At $z_i = 0$

$$\tau_z \dot{z}_i = \tfrac{1}{2}(1 + \tanh(u_i I_i)) > 0,$$

since $\tanh(\cdot) \in (-1, +1)$, strictly for finite I_i. At $z_i = 1$

$$\tau_z \dot{z}_i = -d + \tfrac{1}{2}(1 + \tanh(u_i I_i)) \leq 0,$$

since $d = 1$ and $(1+\tanh(\cdot))/2 \leq 1$. The positive invariance of $(0, 1)$ follows by Nagumo's theorem [13].

(ii) For any fixed B, between consecutive B-switching events, $\mathcal{S}_i, \mathcal{P}_i, \mathcal{C}_i$ are constant, reducing (7) to an ordinary differential equation(ODE) on $(0, 1)$. Applying $\mathrm{sech}^2(\cdot) \leq 1$,

$$\frac{d\dot{z}_i}{dz_i} \leq \frac{-d + u_i \alpha/2}{\tau_z} \begin{cases} < 0 & u_i < u^*, \\ > 0 & u_i > u^*, B = 0. \end{cases}$$

Note: With $u^* = 2d/\alpha$ and $\alpha = 1.5$ in our simulations, u^*=1.33. Hence we take $u_0 = 1.5 > u^*$ for the decision zone. In the evolution zone the bound is strictly negative, so the right-hand side is strictly decreasing. Since $\dot{z}_i|_0 > 0$ and $\dot{z}_i|_1 \leq 0$ from part (i), the intermediate value theorem gives a unique $z_i^* \in (0, 1)$ where $\dot{z}_i = 0$, which is global asymptotically stable: $\dot{z}_i < 0$ for $z_i > z_i^*$ and $\dot{z}_i > 0$ for $z_i < z_i^*$.

(iii) In the decision zone, if $B = \mathbf{0}$, then $I_i = \alpha(z_i - 1/2)$, hence $\dot{z}_i|_{z_i=0.5} = 0$; from the bound above with $\mathrm{sech}^2(0) = 1$, the derivative is strictly positive at $z_i = 0.5$: neutral is unstable, consistent with [12]. For $B \neq 0$, since $\alpha_S > \alpha_P + \alpha_C$ with $\alpha_S > \alpha_P > \alpha_C$ by design, suppression cannot be canceled by permission and coordination combined. Thus, at $z_i = 0.5$

$$I_i = -\alpha_S \mathcal{S}_i + \alpha_P \mathcal{P}_i + \alpha_C \mathcal{C}_i \neq 0.$$

So whenever any conflict channel is active, $z_i = 0.5$ is no longer an equilibrium. At least one equilibrium $z_i^* \in (0, 1)$ exists by (*i*) and the Intermediate Value Theorem. ∎

F.: Predictive Gate and Velocity Optimization

Rather than applying MPC as a monolithic trajectory optimizer, we decompose its two constituent ideas: 1) predictive constraint evaluation drives the commitment gate, determining safe crossing order; and 2) single-step cost minimization drives velocity regulation, ensuring smooth speed adaptation consistent with σ_i, as explained by (4). This decomposition eliminates the need for a quadratic program (QP) solver, preserving the safety guarantees of predictive constraint satisfaction. While the bifurcation phenomenon holds after entering the decision zone as per Proposition 1, the predictive safety gate resolves which direction to take in a hybrid manner: FCFS arrival priority establishes the base ordering, and the feasibility check determines whether that ordering is safely executable or if reordering is possible. On entry to the decision zone, vehicle i records its arrival timestamp t_i^{dz} and broadcasts it via V2V communication alongside the states $(\sigma_i, z_i, \mathbf{x}_i)$. The timestamps $\{t_i^{\mathrm{dz}}\}$ establish a strict FCFS priority ordering: vehicle i evaluates feasibility only after all higher-priority conflicting vehicles ($t_k^{\mathrm{dz}} < t_i^{\mathrm{dz}}$) have committed. When the feasibility check passes, $\sigma_i \to G$ FCFS order is respected. When a higher-priority vehicle decides YIELD and a gap opens, a later-arriving vehicle whose conflict set does not overlap with the current GO vehicle may independently pass feasibility and decide GO, producing a topology-driven reordering.

1) Predictive Feasibility Check: Vehicle i projects its earliest crossing window

$$T_i = \left[t + \tfrac{r_i}{v_i^{\max}},\ t + \tfrac{r_i + L_{\mathrm{box}}}{v_i^{\max}} \right],$$

where $L_{\mathrm{box}} = 2R_{\mathrm{int}} + L_v$. Feasibility requires non-overlapping occupancy windows against all $\sigma_k = G$ neighbors with $K(i, k) = 1$, where $T_i(1)$ and $T_i(2)$ are entry and exit times of vehicle i at the intersection boundary,

$$\min\big(T_i(2), T_k(2)\big) - \max\big(T_i(1), T_k(1)\big) < \varepsilon, \quad \varepsilon = 0.6\,\mathrm{s}. \quad (9)$$

Feasible dcases imply $\sigma_i \to G$, T_i stored and broadcast; infeasible dcases imply $\sigma_i \to Y$. For merge conflicts $M(i, k) = 1$, a time-to-merge-point check with margin $t_{\mathrm{margin}} = 1.5\,\mathrm{s}$ replaces (9). Each commitment event updates $B(k, i)$ for all neighbors via V2V, activating the channels in (8) and inducing an opinion spike among required vehicles, either $z_{k\to 0}$ or $z_{k\to 1}$ mimicking [14]. By construction, no two conflicting vehicles ($K(i, k) = 1$ or $M(i, k) = 1$) hold $\sigma = G$ simultaneously in the intersection zone, since the feasibility check (9) prevents overlapping occupancy windows, guaranteeing collision-free intersection traversal.

Remark 1: Ties in simultaneous t_i^{dz} are broken by vehicle index in simulation. In practice, an approach-direction bias or randomized priority can be injected in such a scenario.

2) Single-Step Multi-Objective Velocity Optimization: Each vehicle tracks its pre-computed path exactly via arc-length parameterization. The optimization layer determines only longitudinal acceleration a_i^* at each timestep solving a multi objective cost function modulated by opinion

$$\begin{aligned} &\underset{a \in \mathcal{A}}{\text{minimize}}\ J_i(a) = J_{\mathrm{prog}} + J_{\mathrm{comf}} + J_{\mathrm{spat}} + J_{\mathrm{yield}} \\ &\text{subject to} \quad a \in [-5.0,\ 2.5]\ \mathrm{m/s^2} \end{aligned}$$

where $\mathcal{A}$ is a uniform grid of $N_c = 15$ candidates over the acceleration limits, which indeed effects the arrival time t_i^{dz} used for decision making. Here, $v_i^{\max} \in \{11.1,\ 8.0,\ 7.0\}\,\mathrm{m/s}$ is the speed limit for straight, left and right maneuvers respectively, ensuring safe cornering speeds across all maneuver types.

a) Progress Cost: Take

$$J_{\text{prog}} = w_p^{(\sigma,z)} \frac{r_i}{\max(v_{\text{pred}}, 0.1)}.$$

The predicted velocity is clipped to a maneuver-dependent speed limit

$$v_{\text{pred}} = \max(0, min(v_i + a\Delta t, v_i^{\max})),$$

where $v_i^{\max}$ reflects the geometric constraint of the assigned maneuver and

$$w_p^{(\sigma,z)} = \begin{cases} 10\, w_p, & \sigma_i = G,\ r_i \le R_{\text{int}}, \\ (0.5 + z_i)\, w_p, & \sigma_i = N, \\ w_p, & \text{otherwise.} \end{cases}$$

In the negotiating state, $z_i \to 1$ (GO) increases approach aggressiveness, while $z_i \to 0$ (YIELD) reduces it, providing a smooth pre-commitment speed adaptation where $w_p = 1$.

b) Comfort Cost: Acceleration effort is penalized quadratically to suppress aggressive maneuvers

$$J_{\text{comf}} = w_c\, a^2, \quad (w_c = 0.5).$$

c) Spatial Repulsion Cost: from conflicting neighbors $K(i,k) = 1$. Let $\mathcal{K}_i = \{k : K(i,k) = 1\}$ denote the set of crossing-conflicting neighbors of vehicle i, and take

$$J_{\text{spat}} = \sum_{k \in \mathcal{K}_i} w_j \, \exp\!\left(-\tfrac{1}{2}(r_{ik} - r_{\text{safe}})\right),$$

$$w_k = \begin{cases} w_{\text{com}} & \sigma_k = G, \\ w_{\text{dec}}\,(0.5 + z_j) & \sigma_k = N,\ r_k < R_{\text{evo}}, \\ w_{\text{evo}} & \text{otherwise.} \end{cases}$$

A negotiating neighbor leaning GO ($z_{k\to 1}$) induces stronger repulsion than one leaning YIELD ($z_{k\to 0}$), reflecting its expressed crossing intent before commitment. J_{spat} is suppressed for crossing conflicts when $\sigma_i = G$ and $r_i \le R_{\text{int}}$, where $w_{com} = 1000$, $w_{dec} = 10$, $w_{evo} = 1$ and the safe distance $r_{safe} = 3$m.

d) Yield Braking Cost: When $\sigma_i = Y$, a braking cost is applied with exponential onset beyond R_{int} ensuring smooth deceleration avoiding discontinuous braking at the stop boundary.

$$J_{\text{yield}} = \begin{cases} w_{\text{com}}\, v_{\text{pred}} & r_i \le R_{\text{int}}, \\ 0.05\, w_{\text{com}}\, v_{\text{pred}}\, e^{-(r_i - R_{\text{int}})/6} & r_i > R_{\text{int}}, \end{cases}$$

IV. Simulation Results and Analysis

We validate the proposed framework in MATLAB across all 80 non-trivial maneuver combinations (out of 81 total combinations, excluding the trivial all-right zero-conflict scenario) involving 4 CAVs at a 4-way unsignalized intersection. All baselines are evaluated under randomized initial conditions across 1200 runs ($d_i = 45 \pm 10$ m, $v_i = 7 \pm 1.5$ m/s). The aggregate last-vehicle exit time is presented in Fig. 3, where n denotes the number of scenarios per conflict type per iteration. The proposed method achieves consistent better average

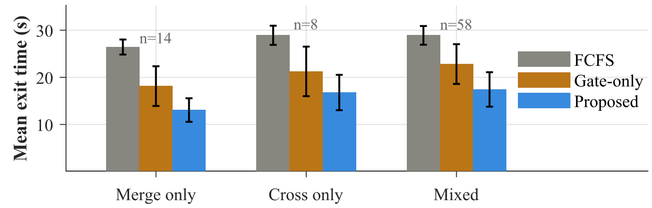

Fig. 3. Mean & deviation (error bar) of last vehicle exit time.

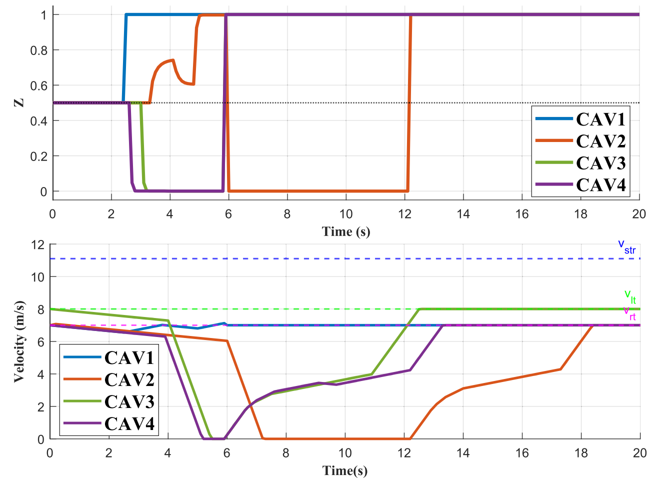

Fig. 4. Scenario 1(mixed maneuvers): (a) z_i; (b) speeds.

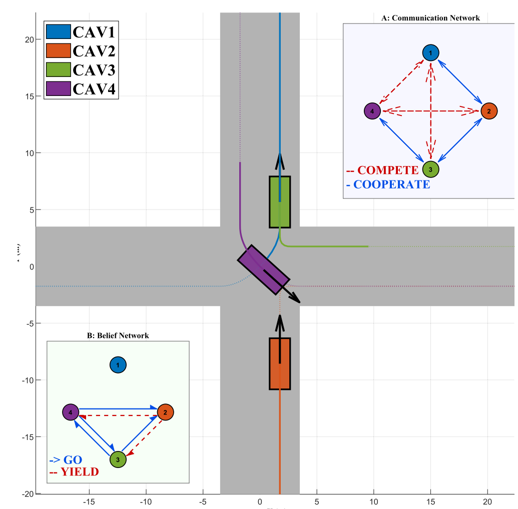

Fig. 5. Scenario 1 snapshots at 9.5s.

TABLE I
Computational Run Times ($N_a = 4$, $\Delta t = 100$ ms)

	MPC	DMPC	Proposed
Solver	NLP	NLP	Grid search
Scales	N_a, N_h	N_h (per veh)	N_c
Mean (ms)	11.93	7.28	2.37

Prediction horizon N_h=5; N_c=15; NLP-non linear programming

performance over strict FCFS and the conflict-aware gate with fixed cost function weights across merge, crossing, and mixed topologies. In TABLE II, 2 representative scenarios are detailed, in Scenario 1, the proposed method approximates FCFS as it is near-optimal and opinion dynamics converge to the same sequence; in Scenario 2, a slight perturbation

TABLE II
SCENARIO CONFIGURATIONS AND LAST VEHICLE EXIT TIMES (S), WHERE CAV ENTRY: (IN-LANE, OUT-LANE, r_i(M), v_i(M/S))

Scenario	CAV1	CAV2	CAV3	CAV4	FCFS (s)	Proposed. (s)
1	(1, 6, 29, 7)	(3, 4, 45, 7)	(5, 6, 50, 8)	(7, 4, 35, 7)	17.09	17.20
2	(1, 6, 29, 7)	(3, 4, 44, 7)	(5, 6, 50, 8)	(7, 4, 35, 7)	17.09	12.50

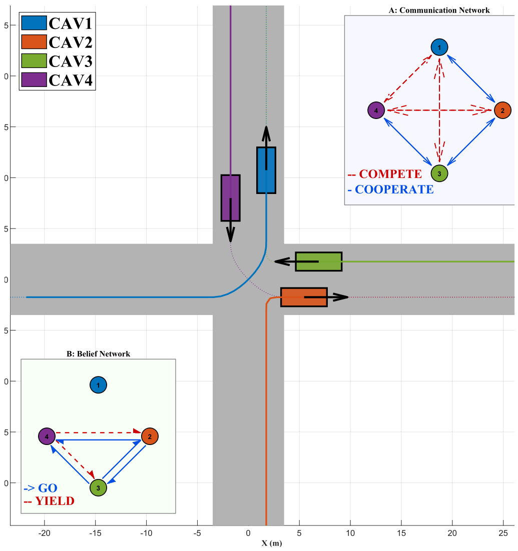

Fig. 6. Scenario 2 (mixed maneuvers) snapshot at 6s.

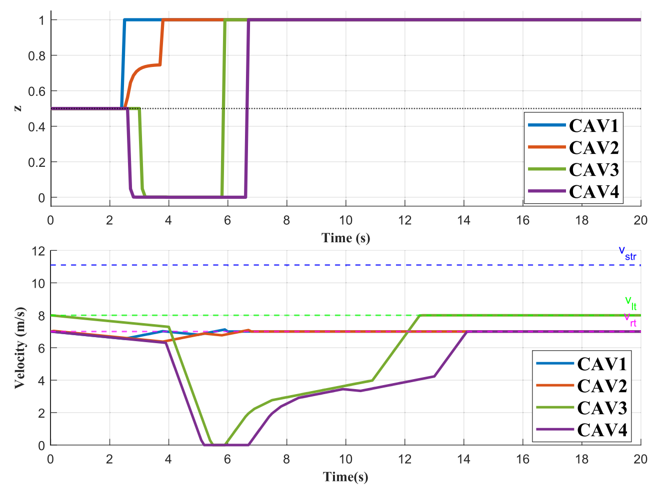

Fig. 7. Scenario 2: (a) z_i; (b) speeds.

of CAV2's initial position creates a feasible gap through heterogeneous conflict sets, enabling an optimal reordering. In the opinion trajectories in Fig. 4 and Fig. 7 we can observe the jump in decision, animated snapshots of CAV2 position and signed graph structure are presented in Fig. 5, Fig. 6.

A. Analysis

TABLE I compares the computational runtimes of our method, MPC, and DMPC. The mean run times per control step are shown when the computations are performed on an Intel i5 processor using MATLAB, with the CasADi tool for performing MPC optimization. Per-vehicle complexity scales as $\mathcal{O}(N_a)$ for the predictive safety gate and opinion ODE. In contrast to MPC, the optimizer scales as $\mathcal{O}(N_c)$, independently of the the number of vehicles and the prediction horizon. The signed graph A can be generalized directly to other intersection lane geometries by recomputing K and M, promising scalability across different intersection types also.

V. CONCLUSION

We have addressed decentralized intersection coordination through a signed-graph opinion dynamics framework, where a conflict topology network and a dynamic belief network jointly drive each vehicle to a GO or YIELD decision without a central coordinator or solver. Our formulation has a lower throughput average than the strict FCFS approach and a conflict aware predictive safety gate policy in crossing, merge, and mixed conflict scenarios with dynamic reordering and it requires less computational time than MPC. Future work will include uncertainty-aware belief updates, stability analysis of the closed-loop decision model across belief switching events, and validating the approach in mixed-traffic environments with higher density and same lane traffic.

REFERENCES

[1] L. Riegger, M. Carlander, N. Lidander, N. Murgovski, and J. Sjöberg, "Centralized MPC for autonomous intersection crossing," in *Proc. IEEE 19th Int. Conf. Intell. Transp. Syst. (ITSC)*, Nov. 2016, pp. 1372–1377.

[2] A. Katriniok, B. Rosarius, and P. Mähönen, "Fully distributed model predictive control of connected automated vehicles in intersections: Theory and vehicle experiments," *IEEE Trans. Intell. Transp. Syst.*, vol. 23, no. 10, pp. 18288–18300, Oct. 2022.

[3] W. Zhong, K. Li, J. Shi, J. Yu, and Y. Luo, "Reservation-prioritization-based mixed-traffic cooperative control at unsignalized intersections," *IEEE Trans. Intell. Vehicles*, vol. 9, no. 5, pp. 4917–4930, May 2024.

[4] M. Khayatian, M. Mehrabian, and A. Shrivastava, "RIM: Robust intersection management for connected autonomous vehicles," in *Proc. IEEE Real-Time Syst. Symp. (RTSS)*, Dec. 2018, pp. 35–44.

[5] Z. Lin, J. Lan, C. Anagnostopoulos, Z. Tian, and D. Flynn, "Safety-critical multi-agent MCTS for mixed traffic coordination at unsignalized intersections," *IEEE Trans. Intell. Transp. Syst.*, vol. 26, no. 11, pp. 18992–19006, Nov. 2025.

[6] X. Gong, B. Wang, and S. Liang, "Collision-free cooperative motion planning and decision-making for connected and automated vehicles at unsignalized intersections," *IEEE Trans. Syst., Man, Cybern., Syst.*, vol. 54, no. 5, pp. 2744–2756, May 2024.

[7] A. Bizyaeva, A. Franci, and N. E. Leonard, "Nonlinear opinion dynamics with tunable sensitivity," *IEEE Trans. Autom. Control*, vol. 68, no. 3, pp. 1415–1430, Mar. 2023.

[8] C. Cathcart, M. Santos, S. Park, and N. E. Leonard, "Proactive opinion-driven robot navigation around human movers," in *Proc. IEEE/RSJ Int. Conf. Intell. Robots Syst. (IROS)*, Oct. 2023, pp. 4052–4058.

[9] T. M. Paine and M. R. Benjamin, "A model for multi-agent autonomy that uses opinion dynamics and multi-objective behavior optimization," in *Proc. IEEE Int. Conf. Robot. Autom. (ICRA)*, May 2024, pp. 8305–8311.

[10] X. Liu, P. Hang, Y. Wang, and J. Sun, "A cooperative decision-making method for CAVs from the perspective of opinion dynamics," *Transp. Res. C Emerg. Technol.*, vol. 182, Jan. 2026, Art. no. 105412.

[11] T. Zaslavsky, "Matrices in the theory of signed simple graphs," 2013, *arXiv:1303.3083*.

[12] A. Bizyaeva, A. Franci, and N. E. Leonard, "Multitopic belief formation through bifurcations over signed social networks," *IEEE Trans. Autom. Control*, vol. 70, no. 8, pp. 5082–5097, Aug. 2025.

[13] F. Blanchini, "Set invariance in control," *Automatica*, vol. 35, no. 11, pp. 1747–1767, Nov. 1999.

[14] C. Cathcart, I. X. Belaustegui, A. Franci, and N. E. Leonard, "Spiking nonlinear opinion dynamics (S-NOD) for agile decision-making," *IEEE Control Syst. Lett.*, vol. 8, pp. 3267–3272, 2024.

Open Access funding provided by 'Libera Università di Bolzano' within the CRUI CARE Agreement